ISSN 0031-918X, Physics of Metals and Metallography, 2019, Vol. 120, No. 8, pp. 782–789. © Pleiades Publishing, Ltd., 2019.
Russian Text © The Author(s), 2019, published in Fizika Metallov i Metallovedenie, 2019, Vol. 120, No. 8, pp. 853–860.

STRUCTURE, PHASE TRANSFORMATIONS, AND DIFFUSION

Dynamic Scenarios of the Formation of Martensite with the {110} Habits in the $Ni_{50}Mn_{50}$ Alloy

M. P. Kashchenko[a, b, *], N. M. Kashchenko[a], V. G. Chashchina[a, b], E. S. Belosludtseva[c], V. G. Pushin[a, c], and A. N. Uksusnikov[c]

[a] *Ural Federal University Named after the First President of Russia B.N. Yeltsin, Ekaterinburg, 620002 Russia*
[b] *Ural State Forestry University, Ekaterinburg, 620100 Russia*
[c] *Mikheev Institute of Metal Physics, Ural Branch, Russian Academy of Sciences, Ekaterinburg, 620990 Russia*
**e-mail: mpk46@mail.ru*

Received February 18, 2019; revised February 19, 2019; accepted March 18, 2019

Abstract—Martensitic transformation $B2-L1_0$ in the ordered alloy $Ni_{50}Mn_{50}$, which occurs at comparatively high temperatures (980–920 K), is discussed with the use of dynamic concepts of the wave control of the threshold deformation. The proximity of the observed orientations of martensite-crystal habits (and of twin boundaries) to the planes of the {110} family makes it possible to use the longitudinal waves along the axes ⟨001⟩ (in the basis of the initial phase) as the driving factors. It is shown that at temperatures of the onset of the transformation there is a satisfactory correspondence between the calculated and experimental data on the tetragonality of martensite and on the volume effect. The opportunity of different dynamic scenarios of the formation of the final phase is noted, namely, of separate crystals; layered structures, in which the crystals of martensite with the identical orientation relationships alternate with the untransformed regions of austenite; and packets of pairwise-twinned crystals. Examples are given of morpho-types corresponding to these scenarios.

Keywords: martensite transformations, dynamic theory, habits, transformation twins, tetragonality, volume effect

DOI: 10.1134/S0031918X19080064

INTRODUCTION

At relatively low temperatures, a phenomenon typical of martensite transformations (MTs) is the formation of martensite crystals possessing a fine internal twin structure (TS), which arises as a consequence of clearly pronounced first-order transitions (for example, in the disordered ferrous alloys [1, 2]) or thermoelastic transformations (for example, in the alloys on the basis of titanium nickelide and many nonferrous alloys [3–5]). The transformation twins, as a rule, represent a totality of alternating regions with the orthogonal (in the initial phase) orientations of principal axes of deformation. Upon the phenomenological crystal-geometric analysis [6–10], the twinning is related to the inhomogeneous deformation necessary to retain the macroscopic invariance of the habit plane; moreover, to a given orientation of the habit there corresponds a well-defined ratio η between the principal and twin components of the TS.

However, experiments [11] showed that the value of η can vary in the limits of one and the same crystal, and there were even untwinned thin-plate crystals or midribs of lens-type crystals fixed in [12, 13]. In the dynamic theory of MTs [14–19], the formation of habits is assumed to be caused by the action of relatively long-wavelength displacements (ℓ waves), and the formation of a TS to be determined in the composition of the control wave process (CWP) by the relatively short-wavelength displacements (*s* waves). Consequently, the orientation of the habit is not connected with the value of η. As the base model, a model of the formation of a regular TS with a coordinated action of *s* and ℓ waves [18, 19] is assumed. The appearance of cooperative wave atomic displacements (in the form of wave beams) is caused by the initial excited (vibrational) states. The ℓ waves produce regions in the form of elongated rectangular parallelepipeds, which are determined by the elastic fields of the dislocation centers of nucleation; and the *s* waves are generated by spontaneously arising excited cells of the crystal lattice upon the optimum (for the realization of the MT) relationship between the phases of the ℓ and *s* vibrations.

The basic component of the TS exists as physically isolated regions, since it is precisely its formation is initiated by, mainly, *s* waves, while the twinned component appears as interlayers between the adjacent basic components (in view of the coherent connection

of the contacting regions of the lattice), i.e., the process of its formation has a subordinate character. The wave vectors of the longitudinal *s* waves are directed along the orthogonal ⟨100⟩ fourfold symmetry axes of the initial phase. In the region of the superimposition of the fronts of the *s* waves, a plane deformation is initiated of the tension–compression type. In the pair of quasi-longitudinal ℓ waves, the first wave ensures the Bain tension ε_{1B} along the third axis of the ⟨100⟩ family. The second ℓ wave initiates compressive deformation, which simultaneously specifies, as the principal axis of compression of the basic component of the TS, that axis of the ⟨100⟩ family that makes the smallest angle with the direction $\mathbf{n}_{2\ell}$ of its wave vector. The induced reproduction of the excited *s* cell (which initially arises spontaneously) in the course of the propagation of the CWP means that the *s* cell nearest to the initial *s* cell appears after the superposition of the *s* waves passes (in the time $T_s/2$, where T_s is the period of *s* vibrations) through the two catheti of the triangle in the directions $[1\bar{1}0]$ and [110], while the hypotenuse of the triangle in the same time is passed at a velocity $v'_{2\ell}$, equal to the projection onto the plane (001) of the velocity $\mathbf{v}_{2\ell}$ of the ℓ wave, which ensures the compressive deformation (see Fig. 1).

On the assumption that both catheti are passed at a velocity $\sqrt{2}v_{s\Delta}$, we obtain a condition

$$v_{s\Delta} = v'_{2\ell}\cos\psi, \tag{1}$$

where ψ is the acute angle between $\mathbf{v}'_{2\ell}$ and $\mathbf{v}_{s\Delta} \parallel \langle 001\rangle$. Within the framework of a harmonic description of the threshold deformation, it is considered, as can be seen from Fig. 1, that the loss of the stability of the lattice of the initial phase, which corresponds to the basic component of the TS, occurs in a region with the transverse size

$$d_s < \lambda_s/2, \quad d_s^* = d_s/\lambda_s < 1/2. \tag{2}$$

It can then be easily ascertained that the following equality is fulfilled for the ratio of the fractions of the components of the TS:

$$\beta_{tw} = 4d_s^* \Big/ \left(1 + \tan\psi - 4d_s^*\right). \tag{3}$$

The model of the formation of a regular TS serves as a basis for the passage to the description of the real distributions of transformation twins, which, as a rule, are fragmented; moreover, each of the fragments can be connected with its own spontaneously emergent active cell [19–22].

It is of interest to establish the possibility of using the developed concepts for the description of high-temperature MTs. In this work, we will discuss the formation of martensite crystals in the $Ni_{50}Mn_{50}$ alloy upon the $B2{-}L1_0$ MT, which possess external and internal boundaries with the orientations close to the planes of the {110} family, using the results of the dynamic theory for a regular TS.

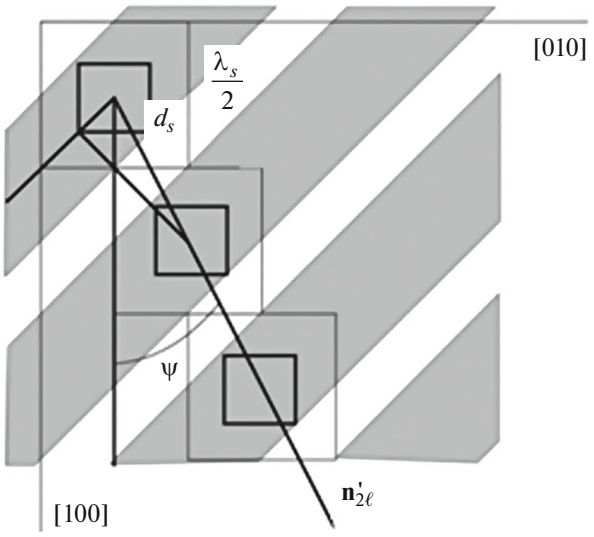

Fig. 1. The dynamic model of the formation of a regular layered (in particular, twin) structure with the ratio of the component portions equal to 2/1 [19].

TETRAGONALITY AND THE VOLUME EFFECT FOR CRYSTALS WITH {110} HABITS

According to [23–28], in the equiatomic ordered alloy $Ni_{50}Mn_{50}$ upon cooling from temperatures exceeding 1000 K, a $B2{-}L1_0$ (or, briefly, β–Θ) MT with the onset temperature $M_s \approx 980$–970 K and finish temperature $M_f \approx 920$ K is observed. The thermal effect, the jump of the electrical resistance, just as a noticeable decrease of the specific (per atom) volume (relative volume effect $\delta \sim -10^{-2}$), make it possible to refer this MTs to the first-order phase transitions; and the highly reversible thermoelastic nature of the MT indicates a sufficiently high degree of the coherence of the contacting phases, which favors the realization of the shape-memory effect.

We will assume that a jumplike change of the state at the M_s temperature is accompanied by a rapid wavelike growth of the thin central part of the martensite crystal (which assigns the orientation of the habit) with the subsequent (in the process of cooling) relatively slow lateral growth. It is clear that in the case of such a mechanism of crystal growth the primary attention upon the comparison of experimental data with the results of calculations is given to the data obtained at the M_s temperature.

The morphological analysis shows that for this MT there are typical crystals with habits close to $\{110\}_\beta$. Further theoretical analysis is carried out for the limiting case of the orientations of boundaries coincident with $\{110\}_\beta$.

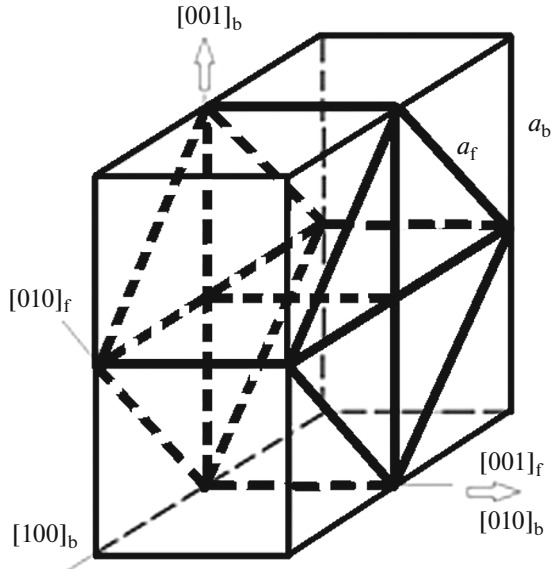

Fig. 2. One of three variants of the selection of the unit cell in the case of Bain deformation of a bcc lattice [3] (subscripts b and f are equivalent to β and to Θ)

If a crystal grows as an isolated object and does not have a fine internal structure consisting of transformation twins, then the description of its morphology is possible in terms of, as a minimum, two dynamic variants [29]. In the first variant, a wave carrier of three-dimensional threshold deformation is considered, which initiates a Bain deformation and leads to a degenerate twin structure (DTS) at $d_s^* = 1/4$, according to (3). The second variant is connected with a wave carrier that initiates plane deformation, supplemented by a deformation in the direction orthogonal to the plane being deformed.

The wave carrier of a three-dimensional threshold deformation that includes a pair of s and a pair of ℓ waves, naturally leads to a two-stage description of deformation (see [18, 29]). The fundamental point is the allowance for the finite deformation after the s stage, which is reflected by the introduction of the coefficient $1 + \varepsilon_{1B}$.

But if the crystals are united into packets of pairwise-twinned crystals, and if the orientation of the boundaries of the packet also belongs to the family $\{110\}_\beta$, then it is natural to interpret the emergent packet as a twinned macrocrystal with an "external" habit, for example, $(101)_\beta$, and "internal" habits (boundaries of the transformation twins), which do not coincide with the "external" habit, for example, $(110)_\beta$ or $(011)_\beta$. The sufficiently large thicknesses of the components of the twin structure are caused by the high-temperature range of the MT, when only the comparatively low-frequency modes entering into the composition of the CWP can be relatively weakly damped.

In principle, a variant of an intermediate layered structure is also possible, in which layers of retained austenite are present instead of the twin component of a macrocrystal.

We, further, assume that the $B2{-}L1_0$ MT is analogous to the bcc–fcc (fct) transformation with the Bain-type deformation, and the designations of the planes and directions refer to the basis of the initial phase, using the symbol β. We assume that the wave process carries the threshold deformation that initiates the Bain deformation (see scheme in Fig. 2): in the four unit cells of the bcc phase (centers of the masses of the atoms are assumed to be located at the vertices and centers of the cubic cells, but are not depicted), the thick lines show the prototype of the fct (or fcc) phase. The principal axis of elongation is oriented along the direction $[010]_\beta \parallel [001]_\Theta$ (edges of the bcc cell); and the principal axes of compression in the equal measure can be selected either along the diagonals of the faces of the bcc cell or along the pair of edges $[100]_\beta$ and $[001]_\beta$. In the latter case, the description of the formation of the basic component of the TS upon the $\beta{-}\Theta$ MT is analogous to the mechanism of the formation of the TS upon the γ(fcc) – α(bcc) MT, and the relationships (1)–(3) do not require any changes.

According to (3), the crystals with the DTS and $\{110\}_\beta$ habits are associated with the following parameters:

$$\psi = 0 \to d_s^* = 1/4. \tag{4}$$

Indeed, the normal $\mathbf{N}$ to the habit plane in the dynamic theory of MTs [16, 17] is reduced to the linear combination of a pair of velocities of ℓ waves:

$$\mathbf{N}_{1,2\ell} \parallel \mathbf{n}_{2\ell} \pm æ_{\ell\ell}\mathbf{n}_{1\ell}, \quad æ_{\ell\ell} = v_{2\ell}/v_{1\ell}, \tag{5}$$

$$|\mathbf{n}_{1,2\ell}| = 1, \quad \mathbf{n}_{1\ell} = \mathbf{v}_{1\ell}/v_{1\ell}, \quad \mathbf{n}_{2\ell} = \mathbf{v}_{2\ell}/v_{2\ell}. \tag{6}$$

Then, in the case of $\psi = 0$ we have

$$\mathbf{n}_{1\ell} = [001]_\beta, \quad \mathbf{n}_{2\ell} = [100]_\beta, \quad N_{1,2\ell} \| [101]_\beta, [10\,{-}1]_\beta. \tag{7}$$

This means that at $\psi = 0$ the CWP includes a pair of longitudinal ℓ waves, one of which propagates along $[001]_\beta$ and carries compressive deformation, and the other propagates along $[100]_\beta$ and carries deformation of elongation. The pair of s waves is similar to those represented in Fig. 1; they propagate along the orthogonal directions of the Δ axes of the fourfold symmetry and carry deformation of the "expansion–compression" type coordinated with the ℓ waves.

At $\psi = 0$, the relationship (1) takes on the form

$$v_{\ell\Delta}/v_{\ell\Sigma} = æ_{\ell s} = 1. \tag{8}$$

It is clear that the condition (8) is easily satisfied in the region of the wave vectors, for which (without an essential loss of accuracy) we can neglect the difference in the velocities caused by the dispersion, for

example, for the wave vectors to $q \sim 0.1q_{max} = 0.2\,\pi/a$, where a is the lattice parameter of the initial phase.

Note that the orientations of the normals

$$\mathbf{N}_{1,2s} \| [110]_\beta, [1\,{-1}0]_\beta \quad (9)$$

to the twinning planes can be trivially found from (6) by the replacements

$$\begin{aligned} æ_{\ell\ell} \to æ_{ss} = 1, \quad \mathbf{n}_{1\ell} \to \mathbf{n}_{1s} = [010]_\beta, \\ \mathbf{n}_{2\ell} \to \mathbf{n}_{2s} = [100]_\beta. \end{aligned} \quad (10)$$

In the case of crystals with habits $(110)_\beta$, the tetragonality t of martensite can easily be related to one of the principal values of the tensor of the Bain deformation.

In the dynamic theory of MTs, the kinematic description of the habit in the threshold regime corresponds to the deformation description. From the requirement of the coincidence of these descriptions, it follows that the ratios of the moduli of deformation of the compression $\varepsilon_2 < 0$ and tension $\varepsilon_1 > 0$ in the threshold regime coincide with the ratios of the squares of the wave velocities:

$$\varepsilon_1/|\varepsilon_2| = (æ_{\ell\ell})^2. \quad (11)$$

Then, it is natural to assume that the austenite lattice, when losing stability and transforming into a state with new stable positions of atoms, preserves the ratio of deformations in the range from the threshold to the finishing values. We additionally assume that the first rapid stage of the transformation is connected with the short-wavelength s deformations (for a time T_s of an order of the period of s vibrations); moreover, it is already at this stage that the finishing Bain (ε_{2B}) deformation of compression in the $[100]_\beta$ direction $\varepsilon_{2s} = \varepsilon_{2B} < 0$ is reached. Since $æ_{ss} = 1$, this means that the tensile deformation along $[010]_\beta$ at the first stage reaches $\varepsilon_{1s} = -\varepsilon_{2s} = -\varepsilon_{2B}$. Since at the second stage (in the time T_ℓ of an order of the period of ℓ vibrations) the compression and the tension are also realized by waves with identical velocities, then the deformation contributions are $\varepsilon_{2\ell} = -\varepsilon_{1\ell}$. From the fct symmetry of the lattice of martensite, it follows that the compressive deformation $\varepsilon_{2\ell}$ along the axis $[001]_\beta$ is equal to the deformation $\varepsilon_{2s} = \varepsilon_{2B}$. Consequently, $\varepsilon_{1\ell} = -\varepsilon_{2B}$, i.e., at the second stage the contribution of the ℓ wave to the main Bain tensile deformation is equal to the contribution from the s wave at the first stage. Let us take into account also that, in view of the inequality $T_\ell \gg T_s$, the ℓ tension acts on the already extended lattice. As a result, the linear dimension a (lattice parameter of the bcc austenite) in the direction $[010]_\beta$ increases by a factor of $(1 + |\varepsilon_{2B}|)^2$, whereas the transverse dimension $a/\sqrt{2}$ decreases by a factor of $(1 - |\varepsilon_{2B}|)$. This means that to determine t we should take the ratio of the edge of the cube of the initial unit cell of the bcc lattice after tensile deformation to the half of the diagonal of the face after compressive deformation:

$$t_\gamma = (1 + |\varepsilon_{2B}|)^2 / \left[(1 - |\varepsilon_{2B}|)\sqrt{2}\right]. \quad (12)$$

According to (12), the tetragonality is absent ($t_\gamma = 1$) if $|\varepsilon^*_{2B}| \approx 0.1173$; $t_\gamma < 1$ at $|\varepsilon_{2B}| < |\varepsilon^*_{2B}|$; and $t_\gamma > 1$ at $|\varepsilon_{2B}| > |\varepsilon^*_{2B}|$. This is illustrated by the data of Table 1.

Table 1. Values of t_γ depending on $-\varepsilon_{2B}$

$-\varepsilon_{2B}$	0	0.11	$-\varepsilon^*_{2B}$	0.12	0.13
t_γ	$1/\sqrt{2}$	0.979	1	1.008	1.038

At the same assumptions, we easily find a relative change in the specific (per atom) volume δ:

$$\delta_\Theta = -\varepsilon^2_{2B}(2 - \varepsilon^2_{2B}) \approx -2\varepsilon^2_{2B} < 0. \quad (13)$$

This means that at $\varepsilon_{2B} \sim 0.1$ the volume effect is $\delta \sim -0.02$.

Strictly speaking, the removal of the degeneracy on the orientations of twinning planes implies the fulfillment of the passage in terms of the values of ψ: $\psi \le 0$ or $\psi \ge 0$.

COMPARISON OF THE CALCULATED AND EXPERIMENTAL DATA

As was noted earlier, the comparison of the data obtained at the M_s temperature is of greatest interest. In the cycle of works [24–28], the data for the temperature dependences of the parameters of the fct martensite lattice a_Θ and c_Θ (and of the tetragonality $t_\Theta = c_\Theta/a_\Theta$) are given in the graphic form in the range from room temperature to 950 K < $M_s \approx$ 980–970 K. If the numerical data of measurements at the temperatures of 900 and 950 K are used for the linear extrapolation, then the following data correspond to the temperature M_{s1} = 980 K: the lattice parameters $a_{\Theta 1} \approx$ 0.389482 nm, $c_{\Theta 1} \approx$ 0.3482 nm; $t_{\Theta 1} \approx$ 0.894; and the specific (per atom) volume $V_{\Theta 1} \approx 0.01320515$ nm^3. For the lattice parameter of the $B2$ phase $a_\beta \approx$ 0.2988 nm, the specific (per atom) volume is $V_\beta \approx 0.01333865$ nm^3 (in the graphs in [24], there is given a somewhat smaller value). Then, we assume as the experimental value

$$\delta_{\Theta,e1} = (V_{\Theta 1} - V_\beta)/V_\beta \approx -0.01001 \ (\approx -1\%).$$

On the other hand, assuming that $t_{\Theta 2} \approx 0.894$ in (12), we find $|\varepsilon_{2B}|_1 \approx 0.07905$ and, substituting $|\varepsilon_{2B}|_1$ into (13), we obtain the following calculated volume effect:

$$\delta_{\Theta,c1} \approx -0.01246 \ (\approx -1.25\%).$$

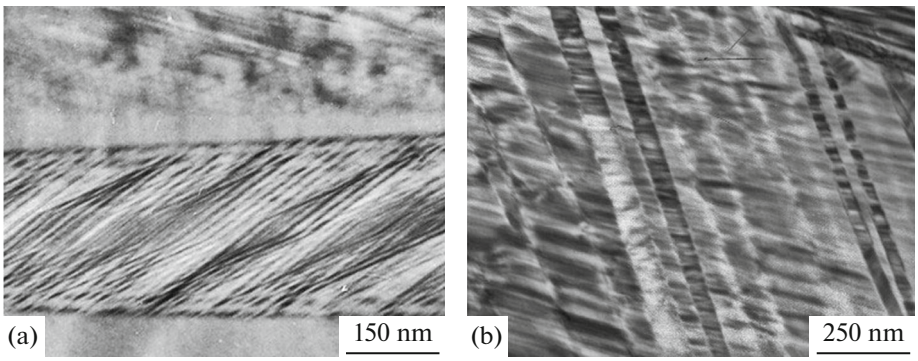

Fig. 3. Typical electron-microscopic images of martensite crystals: (a) an isolated martensite crystal with an internal twin structure; and (b) a packet of martensite crystals with a DTS separated by an APB.

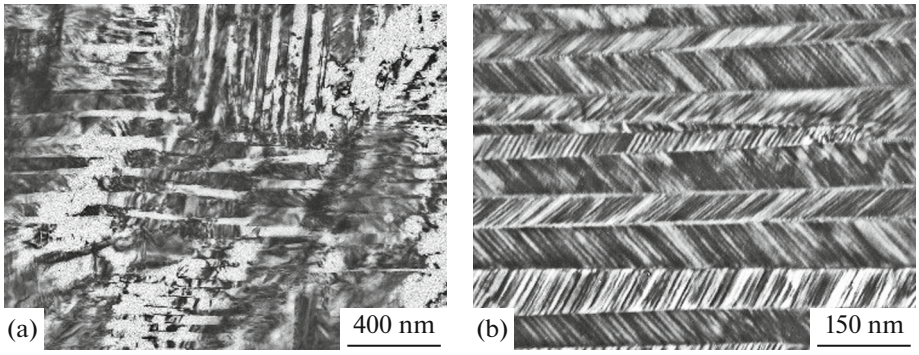

Fig. 4. Typical electron-microscopic images of (a) systems of packets and (b) of a separate packet with a hierarchy of variants of pairwise-twinned martensite crystals.

For the temperature $M_{s2} = 970$ K, we obtain with the same extrapolation:

$a_{\Theta 2} \approx 0.38899 \approx 0.389$ nm, $c_{\Theta 2} \approx 0.3483$ nm, $t_{\Theta 2} \approx 0.8954$,

and then $V_{\Theta 2} \approx 0.01317546$ nm^3 and

$$\delta_{\Theta,e2} \approx -0.01223 \ (\approx -1.22\%). \quad (14)$$

At $t_{\Theta 3} \approx 0.8954$, we find from (12) $|\varepsilon_{2B}|_2 \approx 0.079586$, and from (13)

$$\delta_{\Theta,c2} \approx -0.01263 \ (\approx -1.26\%). \quad (15)$$

The correspondence between the experimental (14) and calculated (15) data appears to be satisfactory.

DISCUSSION OF RESULTS

Note first of all that part of the observed morphological variants of MTs can be compared with the above-noted scenarios (see Figs. 3–5). It is useful to note that in [29] the passage to a DTS permitted an ideal joining of adjacent basic components of the TS. However, in the case of a real discrete lattice, the appearance of inhomogeneities, for example, of antiphase boundaries (APBs) or dislocations, should be expected instead of an ideal joining. In this connection, it cannot be excluded that to the crystal containing an APB shown in Fig. 3 there corresponds a variant of a DTS. The morpho-type shown in Fig. 4 corresponds to a packet consisting of pairs of crystals with alternating twin orientations, which can be considered as a twinned "macrocrystal." Finally, the variant shown in Fig. 5 corresponds to an intermediate layered structure, in which an untransformed initial phase is present instead of the twin component.

Of course, a more complete morphometric analysis of the observed structural variants represents a separate problem. Traditionally of large interest are, for example, the specific features of crystal joints [23].

It is interesting to note that inside the pairwise-twinned large components of the macrocrystal (at least, at room temperatures) nanotwins are also observed, the physical nature of appearance of which requires separate explanation. In [23–27] they are conditionally referred to as "secondary" features. Formally, their appearance can be considered as a consequence of a similar mechanism of dynamic twinning that occurs in a range of shorter-wavelength *s* waves, where the nonlinearity of the dispersion law of phonons in the $\langle 001 \rangle$ directions still can be neglected. In this case, the packet of crystals could be interpreted as

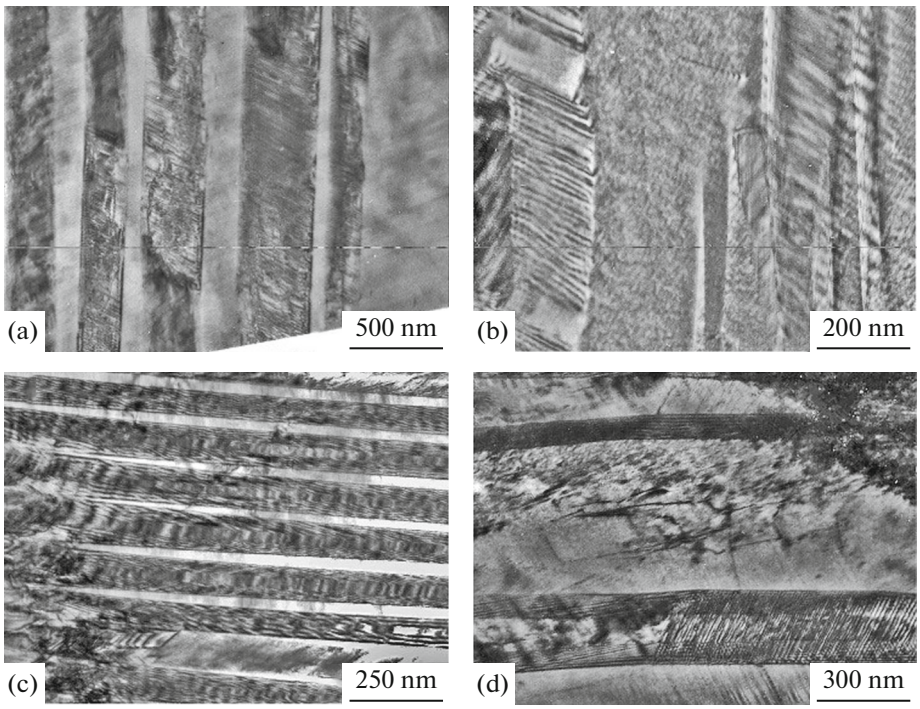

Fig. 5. Typical electron-microscopic images of martensite crystals with a packet morphology, alternating with the layers of (a–c) retained untransformed or (d) reversed austenite.

a hierarchic structure with three scale levels of acting-in-concord purely longitudinal waves with the wave vectors oriented along the fourfold symmetry axes.

However, the appearance of nanotwins via the same dynamic mechanism upon the high-temperature MT is hindered because of the strong damping of short-wavelength displacements. Therefore, in the case of the thicknesses of "secondary" twins on the order of the lattice parameter, their appearance can be caused by the occurrence of a low-temperature accommodation stage of the MT (without a change in the macroscopic morphological features) either via the adaptation of the system to the internal stresses by means of mechanical nanotwinning or by the inheritance of transverse short-wavelength atomic displacements (but with finite frequencies) in the $\langle 110 \rangle$ directions, corresponding to standing waves, which clearly reflect the tendency that appears even in the pretransition state [30, 31].

The satisfactory correspondence between the calculated and experimental values of the volume effect and of the tetragonality (especially, at the temperature $M_s \approx 970$K, corresponding to the larger degree of supercooling below the temperature of the phase equilibrium), apparently, testifies in favor of the wave carrier of three-dimensional threshold deformation. Of course, the transformation itself has a "smeared" nature and it is impossible to separate an only value of M_s.

It is also useful to bear in mind that in the case of the wave carrier initiating plane deformation, not only a uniform deformation can subsequently occur, but also an inhomogeneous short-wavelength (reshuffling) shear [30–33].

CONCLUSIONS

The performed analysis shows that to the martensite crystals with the sets of orientations of the external and internal boundaries close to the planes of the $\{110\}_\beta$ family observed in the $Ni_{50}Mn_{50}$ alloy upon the $B2-L1_0$ MT, in the dynamic theory of MTs there naturally correspond sets of purely longitudinal ℓ and s waves with the wave vectors collinear to $\langle 001 \rangle_\beta$. Part of isolated untwinned crystals can apparently be considered as crystals with a degenerate structure of transformation twins. On the contrary, the packet of pairwise-twinned crystals can be interpreted as a twinned macrocrystal.

The advantageous formation of crystals with the orientations of the boundaries $\{110\}_\beta$ is caused by the opportunity of concordance of the velocities of the ℓ and s waves irrespective of the degree of the elastic anisotropy of crystals over a wide range of wave vectors.

The above variant of the mechanism of a thermoelastic martensitic transformation is supplementary to the usually adopted qualitative variant of the shear-type reconstruction associated with the softest transverse mode.

FUNDING

This work was performed within the framework of the state task of the Ministry of Science and Higher Education of Russia (theme "Struktura," no. AAAA-A18-118020190116-6) and was supported in part by UD RAS (project no. 18-10-2-39) and the Russian Foundation for Basic Research (project no. 18-32-00529 mol_a).

REFERENCES

1. B. A. Bilbi and J. W. Christian, "Martensitic transformations," in *The Mechanism of Phase Transformations in Metals* (London: Institute of Metals, 1956), p. 121–170.
2. G. V. Kurdyumov, L. M. Utevskii, and R. I. Entin, *Transformations in Iron and Steel* (Nauka, Moscow, 1977) [in Russian].
3. H. Warlimont and L. Delay, Martersitic Transformations in Copper-, Silver- and Gold-Based Alloys (Oxford, Pergamon Press, Oxford, 1974; Nauka, Moscow, 1980).
4. K. M. Knowles and D. A. Smith, "The crystallography of the martensitic transformation in equiatomic nickel–titanium," Acta Metall. **29**, 101–110 (1981).
5. S. Miyazaki, K. Otsuka, and C. M. Wayman, "The shape memory mechanism associated with the martensitic transformation in Ti–Ni alloys—I. Self-accommodation," Acta Metall. **37**, 1873–1884 (1989).
6. M. S. Wechsler, D. S. Lieberman, and T. A. Read, "On the theory of the formation of martensite," J. Metals, 1503–1515 (1953).
7. J. S. Bowles and J. K. Mackenzie, "The crystallography of martensite transformations I," Acta Metall. **2**, 129–137 (1954).
8. J. S. Bowles and J. K. Mackenzie, "The crystallography of martensite transformations II," Acta Metall. **2**, 138–147 (1954).
9. J. S. Bowles and J. K. Mackenzie, "The crystallography of martensite transformations III. Face-centered cubic to body-centered tetragonal transformations," Acta Metall. **2**, 224–234 (1954).
10. A. B. Greninger and A. R. Troiano, "The mechanism of martensite formation," Metall. Trans. **185**, 590–598 (1949).
11. T. Maki and C. M. Wayman, "Transformation twin width variation in Fe–Ni and Fe–Ni–C martensites," Proc.1st JIM Int. Symp. on New Aspects of Martensitic Transformation. Suppl. Trans. JIM **17**, 69–74 (1976).
12. V. M. Schastlivtsev, Yu. V. Kaletina, and E. A. Fokina, *Martensitic Transformation in Magnetic Field* (UrO RAN, Ekaterinburg, 2007) [in Russian].
13. V. V. Sagaradze, N. V. Kataeva, I. G. Kabanova, V. A. Zavalishin, A. I. Valiullin, and M. F. Klyukina, "Structural mechanism of reverse $\alpha \rightarrow \gamma$ transformation and strengthening of Fe–Ni alloys," Phys. Met. Metallogr. **115**, 661–671 (2014).
14. M. P. Kashchenko, V. G. Chashchina, and S. V. Vikharev, "Dynamic model of the formation of twinned martensite crystals: I. Control wave process and the removal of degeneracy in twin-boundary orientation," Phys. Met. Metallogr. **110**, 200–209 (2010).
15. M. P. Kashchenko, V. G. Chashchina, and S. V. Vikharev, "Dynamic model of the formation of twinned martensite crystals: II. Pretransition states and relationships between the volumes of the twin components," Phys. Met. Metallogr. **110**, 305–317 (2010).
16. M. P. Kashchenko and V. G. Chashchina, "Dynamic model of supersonic martensitic crystal growth," Phys.-Usp. **54**, 331–349 (2011).
17. M. P. Kashchenko and V. G. Chashchina, "Formation of martensite crystals in the limiting case of a supersonic growth rate," Lett. Mater. **4**, 308–315 (2014).
18. M. P. Kashchenko and V. G. Chashchina, *Dynamic Theory of γ–α Transformation in Iron Based Alloys. Solving the Problem of the Formation of Twinned Martensite Crystals* (Lambert Academic, Saarbrucken, 2012).
19. M. P. Kashchenko, N. M. Kashchenko, and V. G. Chashchina,"Dynamic options for forming transformation twins," Mater. Today: Proc. **4**, 4605–4610 (2017).
20. M. P. Kashchenko and V. G. Chashchina, " Key role of transformation twins in comparison of results of crystal geometric and dynamic analysis for thin-plate martensite," Phys. Met. Metallogr. **114**, 821–825 (2013).
21. M. P. Kashchenko, N. M. Kashchenko, and V. G. Chashchina, " Effect of change in the wavelengths of short wave shifts on the formation of a twin structure fragment in thin lamellar α-martensite crystals," Phys. Met. Metallogr. **119**, 1–5 (2018).
22. M. P. Kashchenko, I. F. Latypov, and V. G. Chashchina, "Correlation of velocities of the waves controlling the thin-plate α-martensite formation and the modulation of the transformation twin structure," Lett. Mater. **7**, 146–150 (2017).
23. K. Adachi and C. M. Wayman, "Electron microscopic study of θ-phase martensite in Ni–Mn alloys," Metall. Trans. A **16**, 1581–1597 (1984).
24. V. G. Pushin, E. S. Belosludtseva, V. A. Kazantsev, and N. I. Kourov, "Features of the martensitic transformation and the fine structure of the intermetallic compound $Ni_{50}Mn_{50}$," Materialovedenie, No. 11, 3–10 (2012).
25. V. G. Pushin, N. N. Kuranova, E. B. Marchenkova, E. S. Belosludtseva, V. A. Kazantsev, and N. I. Kourov, "High-temperature shape memory effect and the $B2-L1_0$ thermoelastic martensitic transformation in Ni–Mn intermetallics," Tech. Phys. **83**, 878–887 (2013).
26. E. S. Belosludtseva, N. N. Kuranova, N. I. Kourov, V. G. Pushin, V. Yu. Stukalov, and A. N. Uksusnikov, "Effect of aluminum alloying on the structure, the phase composition, and the thermoelastic martensitic transformations in ternary Ni–Mn–Al alloys," Tech. Phys. **60**, 1000–1004.
27. E. S. Belosludtseva, N. N. Kuranova, N. I. Kourov, V. G. Pushin, and A. N. Uksusnikov, "Effect of titanium alloying on the structure, the phase composition, and the thermoelastic martensitic transformations in

ternary Ni–Mn–Ti alloys," Tech. Phys. **60**, 1330–1334 (2015).

28. V. G. Pushin, E. S. Belosludtseva, and E. B. Marchenkova, "Multicomponent metallic Ni–Mn-based alloys with thermally, mechanically, and magnetically controlled shape memory effects," Phys. Met. Metallogr. **119**, 1191–1195 (2018).
29. M. P. Kashchenko, N. M. Kashchenko, and V. G. Chashchina, "The formation of martensite crystals with a degenerate structure of transformation twins," Lett. Mater. **8**, 429–434 (2018).
30. V. G. Pushin, V. V. Kondrat'ev, and V. N. Khachin, *Pretransitional Phenomena and Martensitic Transformations* (UrO RAN, Ekaterinburg, 1998) [in Russian].
31. V. A. Lobodyuk, Yu. N. Koval', and V. G. Pushin, "Crystal-structural features of pretransition phenomena and thermoelastic martensitic transformations in alloys of nonferrous metals," Phys. Met. Metallogr. **111**, 165–189 (2011).
32. M. P. Kashchenko and V. G. Chashchina, "Crystal dynamics of the BCC–HCP martensitic transformation: I. Controlling wave process," Phys. Met. Metallogr. **105**, 537–543 (2008).
33. M. P. Kashchenko and V. G. Chashchina, "Crystal dynamics of the BCC–HCP martensitic transformation: II. Morphology," Phys. Met. Metallogr. **106**, 14–23 (2008).

Translated by S. Gorin